

Macromolecules

Volume 42, Number 11

June 9, 2009

© Copyright 2009 by the American Chemical Society

Articles

Exploring the Dithiocarbamate Precursor Route: Observation of a Base Induced Regioregularity Excess in Poly[(2-methoxy-5-(3',7'-dimethyloctyloxy))-1,4-phenylenevinylene] (MDMO-PPV)

Joke Vandenberg,[†] Jimmy Wouters,[†] Peter J. Adriaensens,[†] Raoul Mens,[†] Thomas J. Cleij,[‡] Laurence Lutsen,[‡] and Dirk J. M. Vanderzande^{*,†,‡}

Institute for Materials Research (IMO), Hasselt University, Universitaire Campus, Agoralaan Building D, B-3590 Diepenbeek, Belgium, and Division IMOMECE, IMEC, Universitaire Campus, Wetenschapspark 1, B-3590 Diepenbeek, Belgium

Received February 11, 2009; Revised Manuscript Received April 8, 2009

ABSTRACT: The dithiocarbamate precursor route is a suitable way to synthesize poly(*p*-phenylene vinylene) derivatives in an efficient manner. It is demonstrated that this precursor route combines the straightforward monomer synthesis of the Gilch route with the superior polymer quality of the more complex sulfinyl route. To obtain the polymers, the bisdithiocarbamate MDMO monomer has been polymerized using either lithium bis(trimethylsilyl)amide (LHMDS) or potassium *tert*-butoxide (KtBuO). The addition of either base results in the formation of high molecular weight precursor polymer. It is shown that the polymerization mechanism follows a radical pathway. Furthermore it is demonstrated that the molecular structure of the polymer shows a certain degree of regioregularity when LHMDS is used. The thermal conversion of the precursor polymer into the conjugated system is studied by in situ UV-vis and FT-IR spectroscopy. A NMR study on ¹³C-labeled MDMO-PPV reveals the presence of only a minimal amount of structural defects in the microstructure of the polymer, further confirming the excellent characteristics of the dithiocarbamate precursor route.

Introduction

Nowadays, conjugated polymers find application in various optical and electronic devices such as light emitting diodes (LED),¹ field effect transistors (FET),² photovoltaic cells³ and sensors.⁴ Due to their interesting optoelectronic and electrical properties, a considerable amount of research has been performed on poly(*p*-phenylene vinylene) derivatives (PPV's).¹ PPV's can be synthesized via either direct routes or precursor routes. The most important direct routes make use of step-growth polycondensation reactions, such as Wittig⁵ and Horner⁶ polycondensations, or transition-metal catalyzed coupling reactions such as the Heck⁷ coupling. One of the disadvantages of these

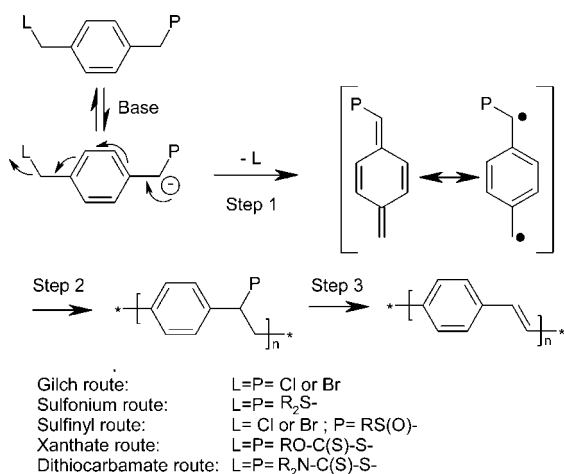
direct routes is that the achieved molecular weights are often significantly lower than those obtained by the precursor routes which make use of the polymerization behavior of *p*-quinodimethane systems. Furthermore, for the direct routes the reaction is very sensitive toward the conditions used and is therefore not easy to control. Four different precursor routes are well described in literature, i.e. the Gilch route,⁸ the Wessling-Zimmerman route,⁹ the xanthate route,¹⁰ and the sulfinyl route.¹¹ The latter is superior because of its versatility, the fact that it can be performed at moderate temperatures in common organic solvents such as alcohols¹² and because it leads to the formation of precursor polymers with extremely low structural defect levels.¹³ Each of these precursor routes makes use of a monomer bearing a polarizer and a leaving group. Via addition of a base, a quinodimethane system, which is the actual monomer, is formed (Scheme 1). Subsequently, this monomer

* Corresponding author. Telephone: +32 (0)11 26 83 21. Fax: +32 (0)11 26 83 01. E-mail: dirk.vanderzande@uhasselt.be.

[†] Institute for Materials Research (IMO), Hasselt University.

[‡] Division IMOMECE, IMEC.

Scheme 1. Precursor Routes toward Poly(*p*-phenylene vinylene) Derivatives



can polymerize into the precursor polymer via a self-initiating radical mechanism.^{14,15} In some cases a competition between this radical mechanism and a certain anionic mechanism^{16,17} is observed, whereby typically the high molecular weight material is associated with the self-initiating radical mechanism and the rather low molecular weight material is produced via an anionic mechanism. In a last step, the precursor polymer is converted into a conjugated material via a thermal or base induced elimination reaction.

Recently our group introduced another precursor route, which also fits to this scheme, the so-called "dithiocarbamate route".¹⁸ Some preliminary studies on the use of the dithiocarbamate precursor route toward the synthesis of poly(thienylene vinylene) (PTV)¹⁹ and poly(*p*-phenylene vinylene) (PPV)²⁰ derivatives have already been reported. However, in both cases it became clear that the polymerization procedure used in this new precursor route still needed to be optimized. Initially lithium diisopropylamide (LDA) was used as the base in these polymerizations. This resulted quite often in the occurrence of side reactions and/or a strong competition between the radical and anionic polymerization mechanism, thus leading to a bimodal molecular weight distribution for the resulting precursor polymer.

This paper presents the use of Lithium-bis(trimethyl)silylamide (LHMDS)²¹ and potassium *tert*-butoxide (K^tBuO) as bases in the dithiocarbamate route toward the synthesis of poly[(2-methoxy-5-(3',7'-dimethyloctyloxy))-1,4-phenylenevinylene] (MDMO-PPV). As will be demonstrated for both bases, precursor polymers are obtained with a monomodal molecular weight distribution, high molecular weight and relative low polydispersities (PD) as compared to the typical PD values observed for the Gilch route.²²

After synthesis and characterization of the precursor polymer, the conversion process toward the conjugated polymer is studied via in situ FT-IR and UV-vis spectroscopy. A NMR study on ¹³C-labeled MDMO-PPV reveals that only a very small amount of defects is present and that the polymerization mainly occurs via head-to-tail additions. Furthermore, a regioregularity excess of 29% in the polymer structure could be calculated through the use of quantitative ¹H NMR. This phenomenon is explained by the steric effects induced by the sterically demanding base LHMDS on deprotonation of the premonomer. For the less sterically hindered base K^tBuO, no regioregular effect is observed.

Experimental Section

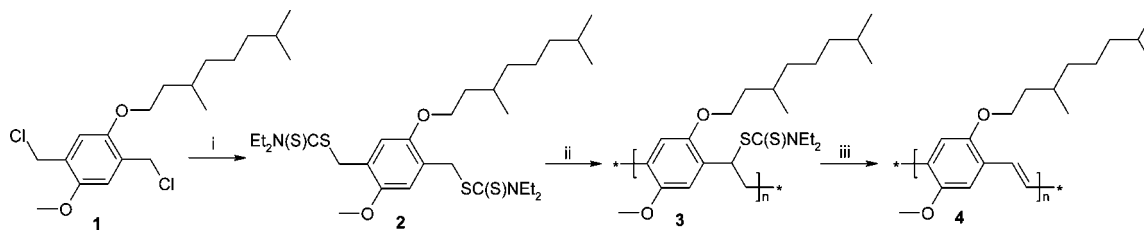
General Data. Unless otherwise stated, all reagents and chemicals were obtained from commercial sources (Acros and Aldrich)

and used without further purification. Tetrahydrofuran (THF) was dried by distillation from sodium/benzophenone. NMR spectra were recorded with a Varian Inova 300 spectrometer at 300 MHz for ¹H NMR and at 75 MHz for ¹³C NMR using a 5 mm probe. Gas chromatography/mass spectrometry (GC/MS) analyses were carried out with TSQ-70 and Voyager mass spectrometers (Thermoquest); the capillary column was a Chrompack Cpsil5CB or Cpsil8CB. Analytical size exclusion chromatography (SEC) was performed using a Spectra series P100 (Spectra Physics) pump equipped with two mixed-B columns (10 μm, 2 cm × 30 cm, Polymer Laboratories) and a refractive index detector (Shodex) at 70 °C. THF was used as the eluent at a flow rate of 1.0 mL/min. Molecular weight distributions are given relative to polystyrene standards. FT-IR spectra were collected with a Perkin-Elmer Spectrum One FT-IR spectrometer (nominal resolution 4 cm⁻¹, summation of 16 scans). UV-vis spectroscopy was performed on a VARIAN CARY 500 UV-vis-NIR spectrophotometer (scan rate: 600 nm/min). Samples for temperature-dependent thin-film FT-IR and UV-vis characterization were prepared by dropcasting the precursor polymer from a CHCl₃ solution (10 mg/mL) onto NaCl disks or quartz disks. The disks were heated in a Harrick high-temperature cell (heating rate: 2 °C/min), which was positioned in the beam of either the FT-IR or the UV-vis spectrometer to allow in situ measurements. Spectra were taken continuously under a continuous flow of N₂ during which the samples were in direct contact with the heating element.

Synthesis. *2,5-Bis(chloromethyl)-1-(3,7-dimethyloctyloxy)-4-methoxybenzene (1)*. Synthesis of 2,5-bis(chloromethyl)-1-(3,7-dimethyloctyloxy)-4-methoxybenzene **1** was reported elsewhere.²³ All properties were in agreement with the previously reported materials.

2,5-Bis(N,N-diethyldithiocarbamate-methyl)-1-(3,7-dimethyloctyloxy)-4-methoxybenzene (2). To 50 mL of an ethanol solution of 2,5-bis(chloromethyl)-1-(3,7-dimethyloctyloxy)-4-methoxybenzene **1** (1 g, 2.767 mmol), sodium diethyldithiocarbamate trihydrate (1.445 g, 6.365 mmol) was added as a solid. The mixture was stirred for 3 h at ambient temperature under a nitrogen atmosphere. Subsequently, 50 mL of water was added and the mixture was filtered over a Buchner to obtain white crystals which were washed with ethanol and water and used without further purification. Yield: 100%. Mp: 70.2–70.7 °C. ¹H NMR (CDCl₃): 6.99 (s, 2H), 4.52 (s, 2H), 4.48 (s, 2H), 3.95 (m, 4H+2H), 3.74 (s, 3H), 3.64 (m, 4H), 1.60–1.85 (m, 2H), 1.38–1.58 (m, 2H), 1.21 (t, 12H), 1.05–1.30 (m, 6H), 0.88 (d, 3H), 0.81 (d, 6H). ¹³C NMR (CDCl₃): 196.11, 195.99, 151.27, 150.90, 125.08, 124.42, 114.75, 113.86, 67.13, 56.19, 49.41, 49.34, 46.61, 39.22, 37.32, 36.83, 36.30, 29.79, 27.95, 24.69, 22.69, 22.59, 19.62, 12.42, 11.59. MS (EI, *m/e*): 148 (M⁺ SC(S)NEt₂), 116 (C(S)NEt₂). IR (NaCl, cm⁻¹): 2954, 2930, 2869, 1485, 1415, 1268, 1207.

Polymerization of 2 (3). In a typical procedure, 500 mg of monomer **2** was dissolved in 4.26 mL of dry THF giving a concentration of 0.2 M. The mixture was stirred at 35 °C under a continuous flow of nitrogen. 1.5 equivalents of either a LHMDS solution (1 M in THF) or a K^tBuO solution (0.87 M in THF) were added in one go to the stirred monomer solution. The reaction proceeded for 1.5 h at 35 °C under a nitrogen atmosphere, and the mixture was subsequently quenched in 100 mL of ice-water. The excess of base was neutralized with HCl (1 M in H₂O). The aqueous phase was extracted with CHCl₃ (3 × 40 mL). After combination of the organic phases and evaporation of the solvent, the obtained crude polymer was again dissolved in 2 mL CHCl₃ and precipitated in 100 mL of stirred cold methanol. The mixture was filtered and the polymer was collected and dried *in vacuo*. The residual fractions contained only monomers and oligomers. Yields: 59%–67%. ¹H NMR (CDCl₃): 6.45–6.97 (br m, 2H), 5.50–5.87 (br s, 1H), 3.05–4.23 (br m, 11H), 1.02–1.95 (br m, 16H), 0.74–1.02 (m, 9H). ¹³C NMR (CDCl₃): 195.76, 150.85 (2C), 127.68 (2C), 114.11, 113.09, 67.10, 56.39, 51.98, 49.08, 46.38, 39.27, 37.54, 36.60, 34.45, 29.91, 27.92, 24.67, 22.69, 22.58, 19.66, 12.47, 11.55. IR (NaCl, cm⁻¹): 2953, 2929, 1504, 1484, 1462, 1413, 1267, 1210,

Scheme 2. Synthesis of MDMO-PPV via the Dithiocarbamate Route^a

^a Key: (i) NaSC(S)NEt₂·0.3H₂O, EtOH; (ii) LHMDS or KtBuO, THF; (iii) ΔT, dichlorobenzene.

1140, 1041.

Thermal Elimination of Precursor Polymer 3 to Conjugated Polymer 4. From a solution of **3** (160 mg) in dichlorobenzene (80 mL) oxygen was removed by purging for 1 h with nitrogen. Subsequently, the solution was heated to 180 °C and stirred for 3 h. After cooling to room temperature, the resulting dichlorobenzene was evaporated and the crude polymer mixture was dissolved in chloroform (2 mL). The solution was precipitated dropwise in cold methanol (100 mL). The polymer was filtered off, washed with cold methanol and dried at room temperature under reduced pressure. The conjugated MDMO-PPV **4** was obtained as a red polymer. The elimination procedure was performed a second time to ensure complete elimination. Yields were quantitative. ¹H NMR (C₂D₂Cl₄): 7.5 (br, 2H) 7.2 (br, 2H) 4.6–3.2 (br m, 5H) 2.1–0.6 (br m; 19H). ¹³C NMR (CDCl₃): 151.4 (2C); 127.0 (2C), 123.3 (2C); 110.5 (1C); 108.8 (1C); 67.9 (1C); 56.4 (1C); 39.2 (1C); 37.4 (1C); 36.6 (1C); 30.2 (1C); 27.9 (1C); 24.6 (1C); 22.6 (2C); 19.8 (1C). IR (KBr, cm⁻¹): 2957, 2925, 2860, 1510, 1469, 1395, 1217, 1028, 872.

Results and Discussion

Monomer Synthesis. The MDMO bisdithiocarbamate monomer **2** is synthesized in one step from the corresponding Gilch bischloromethyl monomer (Scheme 2).¹⁸ The synthetic route toward MDMO Gilch monomer was reported earlier.²³ The dichloride **1** is dissolved in ethanol and solid sodium diethyldithiocarbamate trihydrate is added to the mixture to obtain **2**. The resulting conversion is quantitative. Compared to the synthesis of the MDMO sulfinyl monomer, this one step synthesis is more straightforward.¹¹

Polymerization. The polymerizations of the monomer are performed under nitrogen atmosphere. To this end, the bisdithiocarbamate MDMO monomer **2** is dissolved in dry THF (0.2 M) after which 1.5 equiv of either LHMDS or KtBuO is added as base. After polymerization, the reaction mixture is poured in ice-water, neutralized by hydrochloric acid and extracted with CHCl₃. The polymers are isolated via precipitation in cold methanol. Molecular weights (*M_w*) are determined by GPC relative to polystyrene (PS) standards with THF as the eluent.

In the first series of experiments, the polymerization of monomer **2** is performed with LHMDS as the base at three different temperatures. Increasing the polymerization temperature up to 65 °C leads to precursor polymers with higher polydispersities (PD), and is therefore not favorable. The highest molecular weight is obtained for the precursor polymer synthesized at 35 °C (Table 1). Compared to previous polymerization results, obtained with LDA as base,²⁰ the use of LHMDS strongly suppresses the bimodal molecular weight distribution (Figure 1a). In view of the high molecular weights obtained, it seems that the radical polymerization mechanism^{14,15} is dominating.

To verify whether or not this polymerization reaction follows indeed a radical mechanism, 0.5 equivalents of a radical inhibitor 2,2,6,6-tetramethylpiperinoxyl (TEMPO) were added to a typical

Table 1. Polymerization Results for LHMDS and KtBuO at Different Reaction Temperatures^a

entry	base	temperature (°C)	yield (%)	<i>M_w</i> ^b	PD ^b
1	LHMDS	0	48	138 000	3.2
2	LHMDS	35	64	560 000	3.4
3	LHMDS	65	61	325 000	7.6
4	KtBuO	0	40	238 000	3.3
5	KtBuO	35	67	272 000	2.5
6	KtBuO	65	43	152 000	5.5

^a Data represent average results of two experiments. ^b Determined by means of SEC in THF using polystyrene standards.

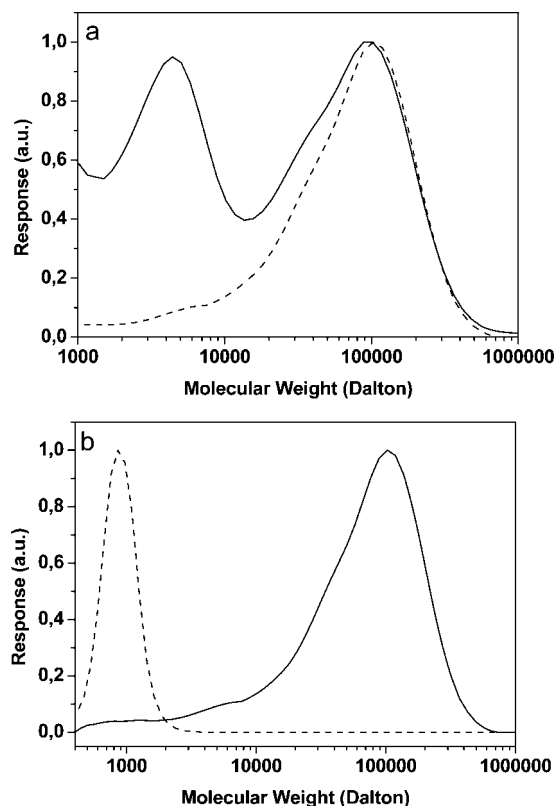


Figure 1. Overlay of SEC chromatograms of precursor polymer **3**. Key: (a) synthesized with LDA (solid line) or with LHMDS (dashed line); (b) synthesized with TEMPO (dashed line) or without TEMPO (solid line).

polymerization mixture (Table 2, Figure 1b). As expected, the addition of TEMPO decreases molecular weight and yield strongly, consistent with a radical polymerization mechanism. In a second experiment, the monomer was added dropwise to a solution of base (Table 2, entry 3), which leads to favorable conditions for an anionic polymerization.²⁴ However, such reversed addition of monomer to base solution has no influence on yield, molecular weight and PD, further confirming the strong preference of this base for a radical polymerization mechanism.

Table 2. Polymerization Results for LHMDS and *K*tBuO at 35 °C under Different Conditions

entry	base	addition	yield (%)	M_w^a	PD ^a
1	LHMDS	normal	59	216 000	2.4
2	LHMDS	TEMPO		1000	1.1
3	LHMDS	reversed	59	234 000	2.4
4	<i>K</i> tBuO	normal	67	272 000	2.5
5	<i>K</i> tBuO	TEMPO		1000	1.1
6	<i>K</i> tBuO	reversed	45	178 000	2.6

^a Determined by means of SEC in THF using polystyrene standards.

When *K*tBuO is used as the base, the polymerization yields again high molecular weight polymer, with the highest value for the precursor polymer synthesized at 35 °C (Table 1). The use of *K*tBuO suppresses the bimodal molecular weight distribution in a similar way as was observed for the LHMDS polymerizations. The experiments with TEMPO and reversed addition also give similar results as was observed for LHMDS as the base (Table 2), indicating once again a preference for a radical polymerization mechanism.^{14,15}

Thermal Conversion. The dithiocarbamate MDMO precursor polymer **3** can be converted into a conjugated material via thermal elimination. Upon heating, the dithiocarbamate groups of precursor polymer **3** are eliminated to form the corresponding conjugated MDMO-PPV **4**. The thermal elimination can be performed in film or in solution. In film, the process can be followed in situ with FT-IR and UV-vis spectroscopy. To perform the elimination in solution, the MDMO precursor polymer is dissolved in dichlorobenzene and heated at 180 °C for 3 h. This procedure is performed two times consecutively, to ensure full conversion.¹³ The polymer is isolated via precipitation in cold methanol.

For the study of the thermal elimination of MDMO precursor polymer **3** with in situ FT-IR and UV-vis spectroscopy, a thin film of precursor polymer **3** was heated at 2 °C/min from ambient temperature to 200 °C under a continuous flow of nitrogen. Upon heating, a new absorption band appears in the UV-vis absorption spectra, associated with the conjugated system (Figure 2a). Concomitantly, the absorption band at 288 nm, associated with the precursor polymer, decreases. The absorption maximum (λ_{\max}) of 460 nm at 134 °C is lower compared to λ_{\max} of 490 nm at room temperature due to the thermochromic effect.²⁵ The elimination process can be more thoroughly analyzed using the absorbance profiles (Figure 2b). In these profiles between 95 and 130 °C, an increase in the absorbance at 460 nm can be noticed under these heating conditions. In the same temperature range, a decrease in the absorbance at 288 nm takes place.

This process can also be monitored using in situ FT-IR spectroscopy. Upon heating, a decrease is observed in the absorption bands at 1205, 1266, 1414, and 1486 cm^{-1} , which arise from vibrations of the dithiocarbamate group²⁶ (Figure 3a). At the same time, a new absorption band appears at 965 cm^{-1} , which originates from the *trans*-vinylene double bonds, formed during thermal elimination. From the FT-IR transmission profiles at 965 and 1266 cm^{-1} , it can be noticed that the elimination starts at 105 °C and is completed at 145 °C, under the heating conditions utilized (Figure 3b). These results are consistent with the UV-vis profiles.

Regioregularity. As the MDMO monomer has a nonsymmetrical structure relative to the position of the OCH_3 and $\text{OC}_{10}\text{H}_{21}$ substituents, upon polymerization typically a random incorporation of both possible quinodimethane systems (1:1) is found.¹³ This has been observed for both the Gilch and the sulfinyl route. It has been previously shown that the degree of regioregularity in MDMO-PPV can be determined by quantitative ¹H NMR analysis using chlorobenzene-*d*₅ as solvent at 100

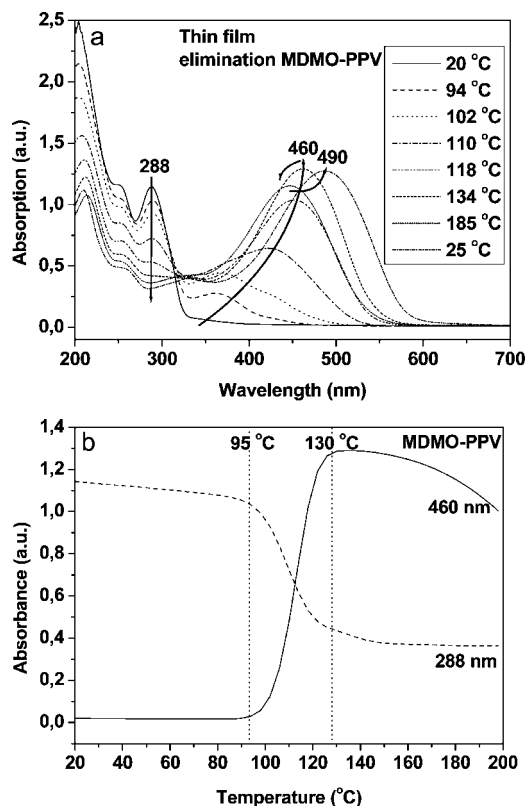


Figure 2. (a) Temperature-dependent UV-vis spectra of the thermal elimination of **3**. (b) UV-vis absorbance profiles at 288 and 460 nm as a function of temperature during the thermal elimination of **3**.

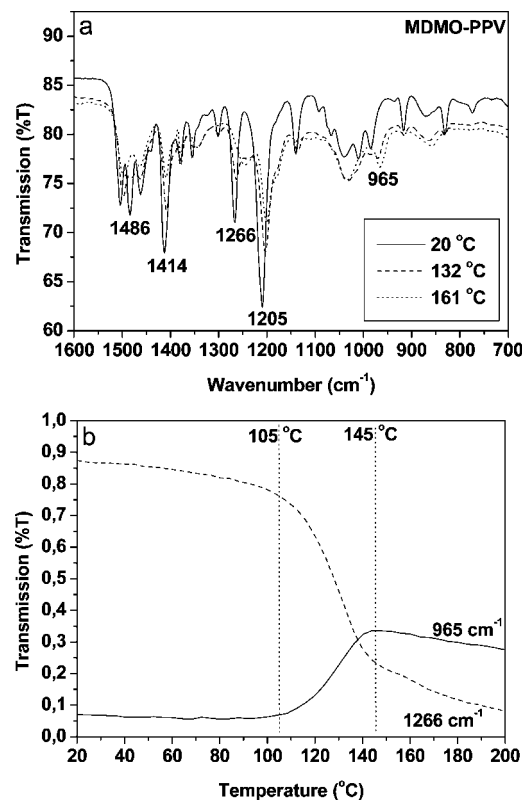
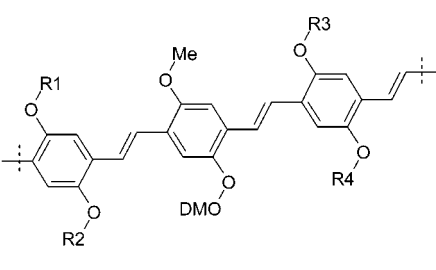


Figure 3. (a) Temperature-dependent FT-IR spectra of the thermal elimination of **3**. (b) IR absorption profiles at 965 and 1266 cm^{-1} as a function of temperature during the thermal elimination of **3**.

°C.²⁷ As the regioregularity may have a profound effect on the opto-electronic characteristics of these materials in devices,²⁸

Chart 1. Representation of Possible Environments for the Methoxy Group in Polymer 4


	R1	R2	R3	R4
A	Me	DMO	DMO	Me
B	DMO	Me	DMO	Me
C	Me	DMO	Me	DMO
D	DMO	Me	Me	DMO

the degree of regioregularity of the MDMO-PPV **4** obtained in our laboratory, was investigated using quantitative ^1H NMR spectroscopy.

In general, irrespectively of the precursor route used, the monomer units in MDMO-PPV can be coupled in 2 ways, creating four different types of environments for the methoxy-groups in the polymer side chain (Chart 1). In the ^1H NMR spectrum of polymer **4**, synthesized with KtBuO , 4 comparable peaks with chemical shifts of 3.98, 3.95, 3.88, and 3.85 ppm can be observed. All these peaks can be assigned to the methoxy-group, indicating a regiorandom MDMO-PPV (Figure 4a). The same peaks can be observed in the ^1H NMR spectrum of polymer **4**, synthesized with LHMDS (Figure 4b). However, for this ^1H NMR spectrum, a quantitative determination of the signal areas using deconvolution reveals that environment C is abundant for 47%, while environments A, B and D are only abundant for respectively 20%, 17%, and 16% (Table 3).

To calculate a degree of regioregularity out of these results, the following formula is used:

$$\% \text{ regioregularity} = x - [(100 - x) \div 3]$$

In this equation, x stands for the % abundance of environment C. In this case, $x = 47\%$, which indicates that the MDMO-PPV polymer prepared with LHMDS exhibits a regioregular excess of 29.3%.

Since the polymerization reaction mainly proceeds via head-to-tail additions, this degree in regioregularity can be explained by the reaction mechanism at the stage of the formation of quinodimethane systems.²⁹ The sterically hindered base LHMDS has a preference to extract a proton at the least sterically hindered position in the premonomer (Scheme 3). The more sterically hindered the base is, the higher this tendency will be. This way, a larger amount of quinodimethane systems is formed with the polarizer directed away from the long alkyl side chain. Due to head-to-tail additions during the propagation step of the polymerization, this results in a 29.3% regioregular MDMO-PPV. The degree of regioregularity in MDMO-PPV synthesized with the less sterically hindered KtBuO , is calculated to be only 2.7%. By using KtBuO , the distribution of quinodimethane systems is reasonably balanced, leading to regiorandom MDMO-PPV.

Quantitative ^{13}C NMR Study. As mentioned before, there are several distinct precursor routes available to synthesize PPV derivatives. The various precursor routes differ from each other in the identity of the functional group that is used as polarizer and leaving group. This chemical differentiation may have an influence on the polymer microstructure, which is a key

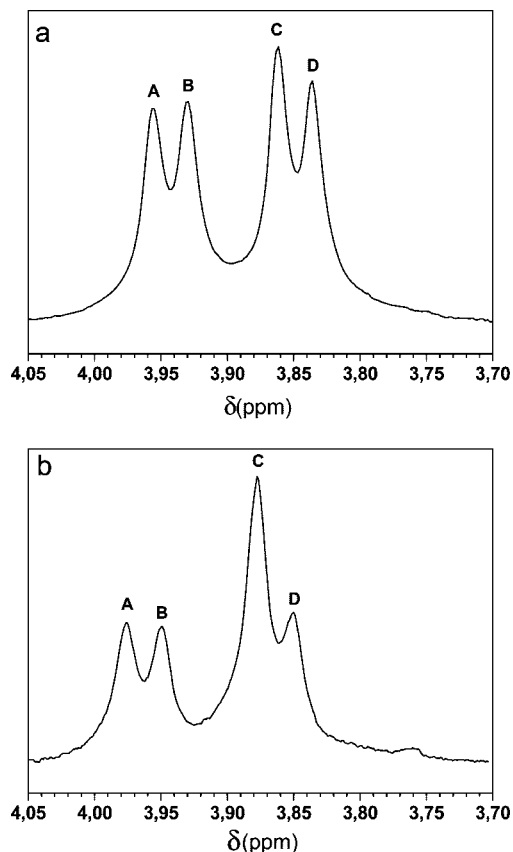


Figure 4. Methoxy region of ^1H NMR spectrum of **4**, measured in chlorobenzene- d_5 at 100 °C. Key: (a) MDMO-PPV synthesized with KtBuO ; (b) MDMO-PPV synthesized with LHMDS.

Table 3. Relative Abundance of Environments A–D in Polymer 4, Synthesized either with LHMDS or with KtBuO

peak	abundance ^a (%)	
	LHMDS	KtBuO
A	20	22
B	17	25
C	47	27
D	16	26

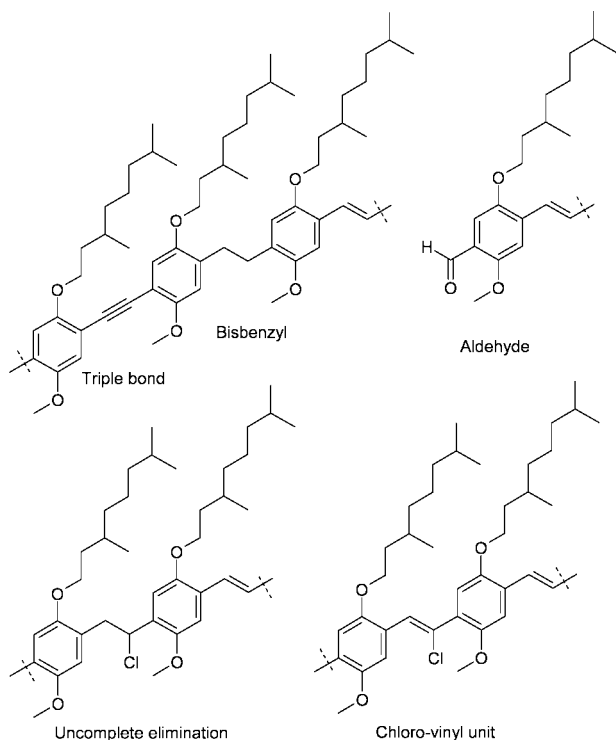
^a Error margin of 1%.

parameter for the polymer performance in electronic devices.^{30,31}

These differences in the microstructure of the PPV polymer can be identified as a consequence of structural defects.³² By definition these defects are an integral part of the polymer microstructure and thus hard to remove or to avoid unless control at high level on the polymerization chemistry can be achieved. By introducing ^{13}C -labels into the polymer chain, the microstructure can be examined via ^{13}C NMR spectroscopy. The NMR study of isotopic labeled polymers is a very powerful technique to gain insight in polymerization mechanisms and resulting polymer structures.^{13,23,33} The microstructure of Gilch-MDMO-PPV has been examined previously by others.²³ Although the concentration of defects in the polymer was very low, by using ^{13}C -labels, the intensity of the defect signals in a ^{13}C NMR spectrum could be increased with a factor 100, making them relatively easy to detect. As main structural defects they found the presence of single and triple bonds, the so-called tolane-bisbenzyl (TBB) moieties (3–4.4%). Later studies¹³ showed even higher quantities of tolane-bisbenzyl defects in Gilch-MDMO-PPV (11.2%) and showed the presence of noneliminated locations (1.8%) as well as chlorovinyl bonds (*ca.* 1.4%), which are a product of tail-to-tail addition (Chart 2). In contrast, only a considerable amount of noneliminated

Table 4. Amounts of Different Types of Structural Defects in MDMO-PPV after First and Second Elimination

defect	first elimination	second elimination
aldehyde	0.6%	0.6%
bisbenzyl unit	0.6%	0.6%
noneliminated groups	<0.1% (detection limit)	<0.1% (detection limit)

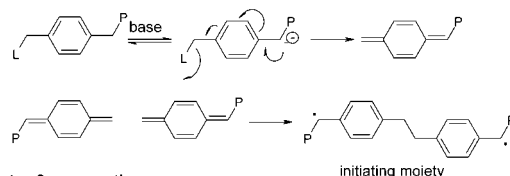
Chart 2. Overview of Different Types of Structural Defects Present in MDMO-PPV Obtained via the Gilch Route

groups was found in the conjugated sulfinyl polymers (6.8%), which could be reduced by a two-step elimination procedure to less than 0.5%. The sulfinyl polymer contained besides the noneliminated groups no other defects, except for aldehyde end groups and the bisbenzyl initiation defect.

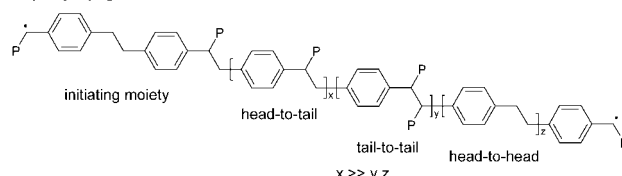
To obtain a profound insight into the microstructure of MDMO-PPV, synthesized via the dithiocarbamate route, a similar ^{13}C NMR study was initiated. As mentioned earlier, the dithiocarbamate route follows a free radical polymerization mechanism. The initiating moiety is a diradical (Scheme 4, step 1), which can at both sides propagate independently via reaction with *p*-quinodimethane intermediates (Scheme 4, step 2). It is expected that this mainly happens via head-to-tail additions, creating a regular polymer chain. During the propagation step

Scheme 4. Radical Precursor Polymerization Mechanism for MDMO-PPV^a

step 1: formation of *p*-quinodimethane systems and subsequent initiation

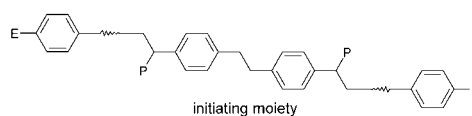


step 2: propagation



note: only one propagating chain end is mentioned

step 3: termination

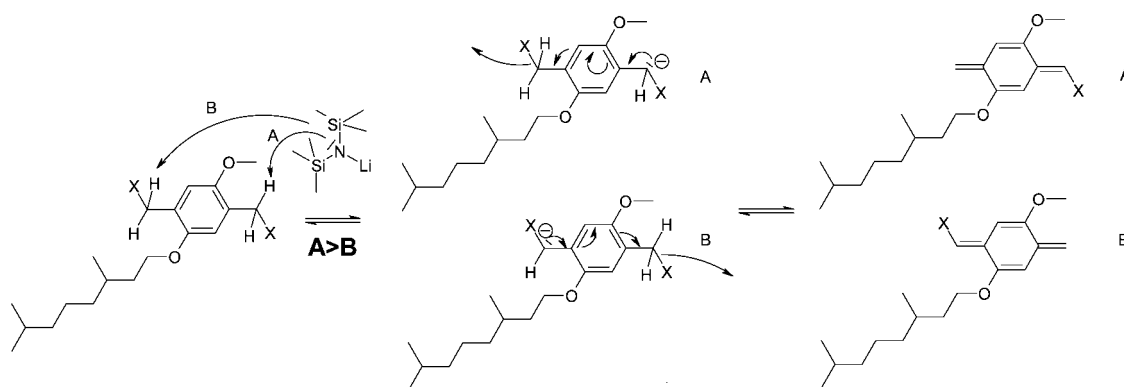


^a L = SC(S)NR₂, P = SC(S)NR₂, and E = C(O)H or C(O)OH.

however, defects can be built in by head-to-head addition leading to a CH₂-CH₂ defect, while tail-to-tail addition causes the formation of a CHSC(S)NR₂-CHSC(S)NR₂ defect. For the termination reaction (Scheme 4, step 3), it is proposed that carbonyl formation by traces of oxygen can take place. As noted previously, after polymerization the precursor polymer chain is converted to the conjugated polymer by thermal elimination.

For this study, the ^{13}C -labeled MDMO-PPV was synthesized using the dithiocarbamate route (Scheme 5). The ^{13}C -labeled bischloromethyl monomer was converted to the corresponding ^{13}C -bisdithiocarbamate monomer, which polymerized under the influence of LHMDS. The precursor polymer was then converted into the conjugated ^{13}C -labeled MDMO-PPV.

Quantitative ^{13}C NMR spectra are necessary to examine the nature and exact amount of structural defects in a polymers microstructure. To acquire quantitative ^{13}C NMR spectra, a preparation delay of five times the longest T1 relaxation decay time has to be respected between consecutive pulses, in order to let the magnetization return to equilibrium. The T1 decay times of all carbon resonances in MDMO-PPV have already been determined previously by means of the inversion recovery technique.¹³ The influence of varying concentrations of the paramagnetic relaxation agent chromium(III) acetylacetonate on the T1 relaxation decay times was investigated. The longest T1

Scheme 3. Formation of Quinodimethane Systems out of MDMO Premonomer, X = SC(S)NR₂

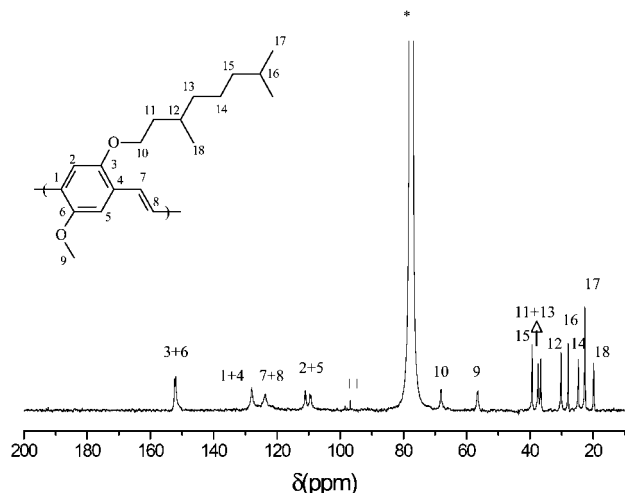


Figure 5. ^{13}C NMR spectrum of unlabeled MDMO-PPV at 40 °C. The resonances marked with an asterisk and a square result from CDCl_3 and CCl_4 respectively. ^{13}C NMR (100 MHz, CDCl_3): $\delta = 151.4$ (C_{3+6} , 2C); 127.0 (C_{1+4} , 2C), 123.3 (C_{7+8} , 2C); 110.5 (C_2 , 1C); 108.8 (C_5 , 1C); 67.9 (C_{10} , 1C); 56.4 (C_9 , 1C); 39.2 (C_{15} , 1C); 37.4 (C_{13} , 1C); 36.6 (C_{11} , 1C); 30.2 (C_{12} , 1C); 27.9 (C_{16} , 1C); 24.6 (C_{14} , 1C); 22.6 (C_{17} , 2C); 19.8 (C_{18} , 1C).

relaxation decay time in the presence of 25 mM of chromium(III) acetylacetonate was determined to be 1.0 s, allowing acquisition of quantitative data with a preparation delay of only 5.0 s.

By comparing the ^{13}C NMR spectra of the unlabeled (Figure 5) and labeled (Figure 6) conjugated MDMO-PPV obtained via the dithiocarbamate route, some additional resonances could be detected. These resonances were situated at 189.1 ppm and a downfield shoulder at 31 ppm. Because these resonances are not detected in the ^{13}C NMR spectrum of the unlabeled polymer, it is likely that they are present in amounts less than 10%. A summed integration of a selection of well-defined carbon signals (carbon atom 3, 6, 17, and 18) was taken as an internal reference, to which the other resonances were normalized. In this way, the amount of every type of structural defect could be quantified from the ^{13}C NMR spectra. The signal at 189.1 ppm can be attributed to an aldehyde functionality (0.6%). This defect was also found with the Gilch (0.1%) and sulfinyl route (0.3%). Since OC_{10} -PPV is stable up to about 175 °C,³⁴ this functionality can be assigned to the end groups of the polymer. The intensity of the aldehyde signal did not change after performing a second elimination (Table 4). Furthermore, the aldehyde signal is also detected in the ^{13}C NMR spectrum of the labeled precursor polymer (Figure 7). This verifies that the origin of the aldehyde end groups lies not at the elimination step at relative high temperature, but rather at the termination reaction of traces of oxygen with the radical ends of the polymer chain during polymerization.

The only other defect visible can be found as a shoulder at 31 ppm, which can be attributed to a bisbenzyl unit (0.6%). Since no $\text{CHSC}(\text{S})\text{NR}_2$ - $\text{CHSC}(\text{S})\text{NR}_2$ tail-to-tail defects and

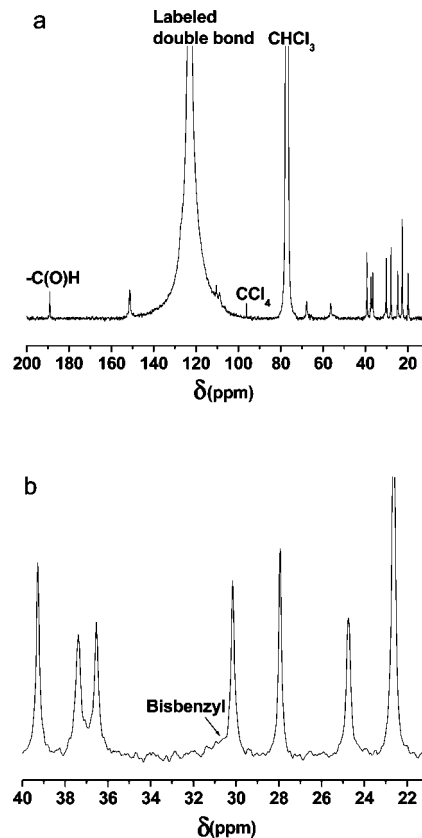


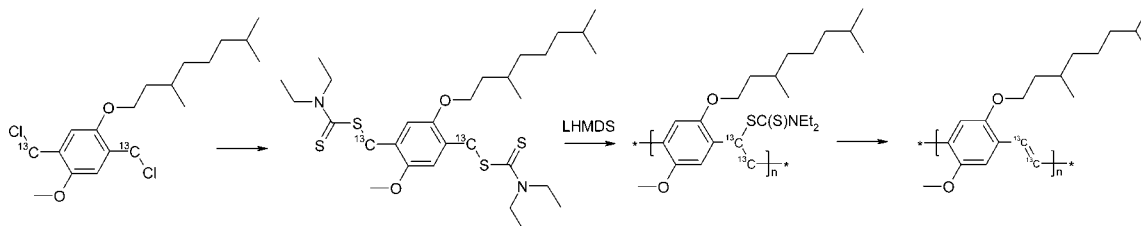
Figure 6. (a) ^{13}C NMR spectrum of labeled dithiocarbamate MDMO-PPV after second elimination. (b) Enlargement of labeled dithiocarbamate MDMO-PPV ^{13}C NMR spectrum between 21 and 40 ppm.

no triple bonds were observed, all bisbenzyl units originate from the initiating moieties and not from head-to-head couplings (Scheme 4). Furthermore, the absence of $\text{CHSC}(\text{S})\text{NR}_2$ - $\text{CHSC}(\text{S})\text{NR}_2$ defects as well as triple bonds leads to the conclusion that recombination of two growing radical chain termini, as was proposed for the Gilch route,³⁵ is not observed for the dithiocarbamate route. Interestingly, the amount of both aldehyde and bisbenzyl initiation units are the same, indicating that all polymer end groups are aldehyde functionalities. Finally, no noneliminated groups could be found at this detection level (<0.1%) and no *cis*-vinylene bonds were observed with ^1H NMR (Supporting Information). Hence, we can conclude that also the dithiocarbamate route leads to polymers with very few microstructural defects.

Conclusions

The synthesis of high quality MDMO-PPV with the dithiocarbamate route has been demonstrated. The use of LHMDS or *K*tBuO as a base, results in polymers with high molecular weight, low PD, and sufficient high λ_{max} values. Contrary to LDA-based dithiocarbamate polymerizations, no bimodal mo-

Scheme 5. Reaction Sequence for the Synthesis of ^{13}C -Labeled MDMO-PPV with the Dithiocarbamate Route



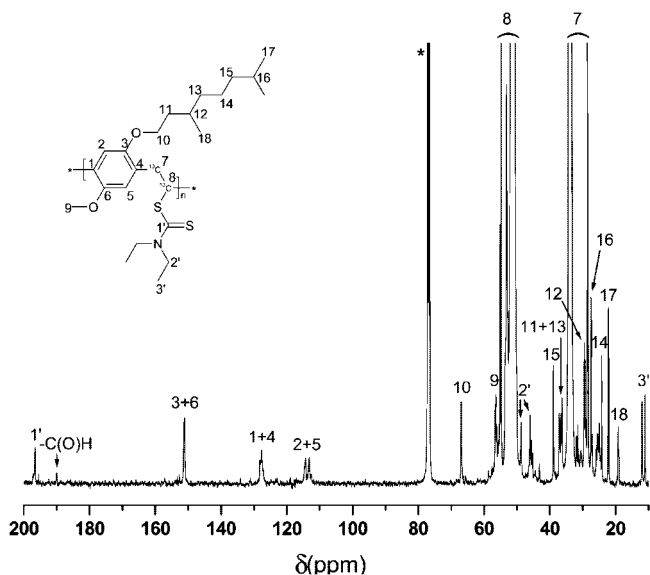


Figure 7. ^{13}C NMR spectrum of labeled precursor MDMO-PPV at 40 °C. The resonance marked with an asterisk results from CDCl_3 ^{13}C NMR (100 MHz, CDCl_3), $\delta = 197.5$ (C_1 , 1C); 151.4 (C_{3+6} , 2C); 127.0 (C_{1+4} , 2C); 115.5 (C_{2+5} , 2C); 67.9 (C_{10} , 1C); 56.4 (C_9 , 1C); 55.5–50.5 (C_8 , 1C); 48.3 (C_2 , 2C); 39.2 (C_{15} , 1C); 37.0 (C_{13+11} , 2C); 35.7–29.3 (C_7 , 1C); 30.2 (C_{12} , 1C); 27.9 (C_{16} , 1C); 24.6 (C_{14} , 1C); 22.6 (C_{17} , 2C); 19.8 (C_{18} , 1C); 11.6 (C_3 , 2C).

lecular weight distributions are obtained. Furthermore, the dithiocarbamate monomer is more readily synthesized than the sulfinyl monomer. Unlike the Gilch route, ^{13}C NMR studies have shown that polymerization of bisdithiocarbamate monomers mainly proceeds via head-to-tail additions and only very small amounts of defects are present in the resulting microstructure. These results prove that the dithiocarbamate route is an optimal balance between the straightforwardness of the Gilch route and the excellent material qualities of the sulfinyl route. Furthermore, MDMO-PPV synthesized with LHMSDS shows a 29.3% regioregularity excess, as revealed by ^1H NMR. By using even more sterically hindered bases, there is potential to synthesize PPV's with even higher degrees of regioregularity.

Acknowledgment. The authors thank H. Penxten for the in situ UV-vis and FT-IR measurements. The authors gratefully acknowledge The Fund for Scientific Research-Flanders (FWO) and the BELSPO in the frame of network IAP P6/27, for the financial support. We also thank the IWT (Institute for the Promotion of Innovation by Science and Technology in Flanders) for the financial support via the SBO project "Polyspec".

Supporting Information Available: Figures showing the raw ^{13}C NMR spectrum of ^{13}C -labeled dithiocarbamate monomer **2** and the raw ^1H NMR spectrum of unlabeled MDMO-PPV **4**. This material is available free of charge via the Internet at <http://pubs.acs.org>.

References and Notes

- (1) Kraft, A.; Grimsdale, A. C.; Holmes, A. B. *Angew. Chem., Int. Ed.* **1998**, *37*, 403–428.

- (2) Dimitrakopoulos, C. D.; Mascaro, D. J. *IBM J. Res. Dev.* **2001**, *45*, 11–27.
- (3) Nunzi, J.-M. *C. R. Phys.* **2002**, *3*, 523–542.
- (4) MacDiarmid, A. G.; Zhang, W. J.; Huang, Z.; Wang, P. C.; Huang, F.; Xie, S. *Polym. Prepr.* **1997**, *38*, 333–334.
- (5) Hörhold, H.-H.; Opfermann, J. *Macromol. Chem.* **1970**, *131*, 105–132.
- (6) Pfeiffer, S.; Hörhold, H.-H. *Synth. Met.* **1999**, *101*, 109–110.
- (7) Heitz, W.; Brüggling, W.; Freund, L.; Gailberger, M.; Greiner, A.; Jung, H.; Kampschulte, U.; Nießner, N.; Osan, F.; Schmidt, H.-W.; Wicker, M. *Macromol. Chem.* **1988**, *189*, 119–127.
- (8) Gilch, H. G.; Wheelwright, W. L. *J. Polym. Sci.* **1966**, *4*, 1337–1349.
- (9) Wessling, R. A. *J. Polym. Sci., Polym. Symp.* **1985**, *72*, 55–66.
- (10) Son, S.; Dodabalapur, A.; Lovinger, A. J.; Galvin, M. E. *Science* **1995**, *269*, 376–378.
- (11) Louwet, F.; Vanderzande, D.; Gelan, J. *Synth. Met.* **1995**, *69*, 509–510.
- (12) Van Breemen, A. J. J. M.; Issaris, A. C. J.; de Kok, M. M.; Van Der Borgh, M. J. A. N.; Adriaensens, P. J.; Gelan, J. M. J. V.; Vanderzande, D. J. M. *Macromolecules* **1999**, *32*, 5728–5735.
- (13) Roex, H.; Adriaensens, P.; Vanderzande, D.; Gelan, J. *Macromolecules* **2003**, *36*, 5613–5612.
- (14) Wiesecke, J.; Rehahn, M. *Angew. Chem., Int. Ed.* **2003**, *42*, 567–570.
- (15) Schwalm, T.; Wiesecke, J.; Immel, S.; Rehahn, M. *Macromolecules* **2007**, *40*, 8842–8854.
- (16) Hontis, L.; Van Der Borgh, M.; Vanderzande, D.; Gelan, J. *Polymer* **1999**, *40*, 6615–6617.
- (17) Adriaensens, P.; Van der Borgh, M.; Hontis, L.; Issaris, A.; van Breemen, A.; de Kok, M.; Vanderzande, D.; Gelan, J. *Polymer* **2000**, *41*, 7003–7009.
- (18) Henckens, A.; Lutsen, L.; Vanderzande, D.; Knipper, M.; Manca, J.; Aernouts, T.; Poortmans, J. *SPIE Proc.* **2004**, 52–59.
- (19) Henckens, A.; Colladet, K.; Fourier, S.; Cleij, T. J.; Lutsen, L.; Gelan, J. *Macromolecules* **2005**, *38*, 19–26.
- (20) Henckens, A.; Duyssens, L.; Lutsen, L.; Vanderzande, D.; Cleij, T. J. *Polymer* **2006**, *47*, 123–131.
- (21) Banishoeb, F.; Adriaensens, P.; Berson, S.; Guillerez, S.; Douheret, O.; Manca, J.; Fourier, S.; Cleij, T. J.; Lutsen, L.; Vanderzande, D. *Solar Energy Mater. Solar Cells* **2007**, *91*, 1026–1034.
- (22) Hontis, L.; Vrindts, V.; Vanderzande, D.; Lutsen, L. *Macromolecules* **2003**, *36*, 3035–3044.
- (23) Becker, H.; Spreitzer, H.; Ibrom, K.; Kreuder, W. *Macromolecules* **1999**, *32*, 4925–4932.
- (24) Neef, C. J.; Ferraris, J. P. *Macromolecules* **2000**, *33*, 2311–2314.
- (25) Kesters, E.; Vanderzande, D.; Lutsen, L.; Penxten, H.; Carleer, R. *Macromolecules* **2005**, *38*, 1141–1147.
- (26) Chambon, S.; Rivaton, A.; Gardette, J.-L.; Firon, M.; Lutsen, L. *J. Polym. Sci., Part A: Polym. Chem.* **2007**, *45*, 317–331.
- (27) Suzuki, Y.; Hashimoto, K.; Tajima, K. *Macromolecules* **2007**, *40*, 6521–6528.
- (28) Mozer, A. J.; Denk, P.; Scharber, M. C.; Neugebauer, H.; Sariciftci, N. S.; Wagner, P.; Lutsen, L.; Vanderzande, D.; Kadashchuk, A.; Staneva, R.; Resel, R. *Synth. Met.* **2005**, *153*, 81–84.
- (29) Wiesecke, J.; Rehahn, M. *Macromol. Rapid Commun.* **2007**, *28*, 188–193.
- (30) Lutsen, L.; Adriaensens, P.; Becker, H.; Van Breemen, A. J.; Vanderzande, D.; Gelan, J. *Macromolecules* **1999**, *32*, 6517–6525.
- (31) Munters, T.; Martens, T.; Goris, L.; Vrindts, V.; Manca, J.; Lutsen, L.; DeCeuninck, W.; Vanderzande, D.; De Schepper, L.; Gelan, J.; Sariciftci, N. S.; Brabec, C. J. *Thin Solid Films* **2002**, *403–404*, 247–251.
- (32) Schoor, H. F. M.; Demandt, R. J. C. E. *Philips J. Res.* **1998**, *51*, 527–533.
- (33) Bjerring, M.; Nielsen, J. S.; Nielsen, N. C.; Krebs, F. C. *Macromolecules* **2007**, *40*, 6012–6013.
- (34) Kesters, E.; Lutsen, L.; Vanderzande, D.; Gelan, J.; Nguyen, T. P.; Molin, P. *Thin Solid Films* **2002**, *403–404*, 120–125.
- (35) Schwalm, T.; Rehahn, M. *Macromol. Rapid Commun.* **2008**, *29*, 207–213.

MA9003105